Optogenetic stimulation of multiwell MEA plates for neural and cardiac applications

Isaac P. Clements*[a], Daniel C. Millard[a], Anthony M. Nicolini[a], Amanda J. Preyer[a], Robert Grier[a], Andrew Heckerling[a], Richard A. Blum[a], Phillip Tyler[a], K. Melodi McSweeney[b], Yi-Fan Lu[b], Diana Hall[b], James D. Ross[a],

[a]Axion Biosystems, 1819 Peachtree Rd. Ste. 350, Atlanta, GA 30309; [b] Institute for Genomic Medicine, Columbia University Medical Center, 630 W 168th St New York, NY 10032;

ABSTRACT

Microelectrode array (MEA) technology enables advanced drug screening and "disease-in-a-dish" modeling by measuring the electrical activity of cultured networks of neural or cardiac cells. Recent developments in human stem cell technologies, advancements in genetic models, and regulatory initiatives for drug screening have increased the demand for MEA-based assays. In response, Axion Biosystems previously developed a multiwell MEA platform, providing up to 96 MEA culture wells arrayed into a standard microplate format.

Multiwell MEA-based assays would be further enhanced by optogenetic stimulation, which enables selective excitation and inhibition of targeted cell types. This capability for selective control over cell culture states would allow finer pacing and probing of cell networks for more reliable and complete characterization of complex network dynamics.

Here we describe a system for independent optogenetic stimulation of each well of a 48-well MEA plate. The system enables finely graded control of light delivery during simultaneous recording of network activity in each well. Using human induced pluripotent stem cell (hiPSC) derived cardiomyocytes and rodent primary neuronal cultures, we demonstrate high channel-count light-based excitation and suppression in several proof-of-concept experimental models. Our findings demonstrate advantages of combining multiwell optical stimulation and MEA recording for applications including cardiac safety screening, neural toxicity assessment, and advanced characterization of complex neuronal diseases.

Keywords: optogenetics, microelectrode array, *in vitro*, induced pluripotent stem cells, disease-in-a-dish, cardiac safety

1. INTRODUCTION

MEA technology supports cell based assays and phenotypic disease modeling

MEAs provide a non-invasive platform for recording electrical activity from cultured neurons or cardiac cells (Fig. 1). Analysis of activity from cells distributed across a culture produces network activity metrics such as excitability, synchrony, and cardiac beat rate. These types of metrics are critical for assessing the effects of experimental conditions such as potential therapeutics, toxins, or cell culture variations including genetic edits. As a result, MEAs are used in a range of applications, including disease modeling[1,2], drug screening[3,4], safety pharmacology[5,6,7], and neural circuit investigation[8].
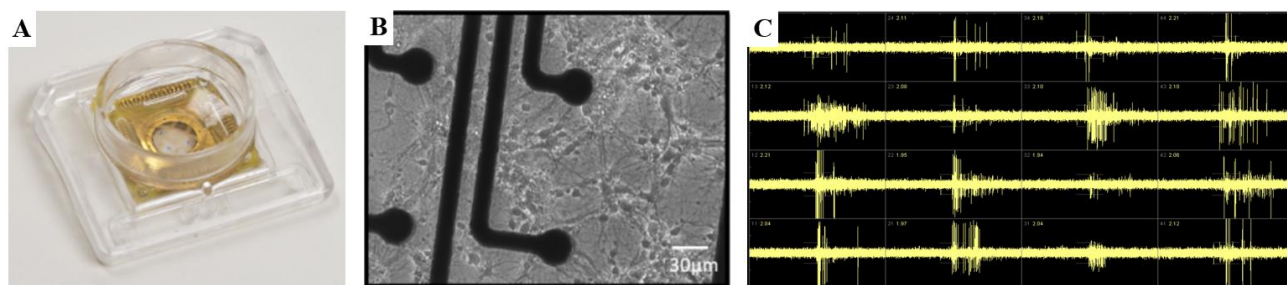
Figure 1. (A) Example MEA culture well (B) A grid of microelectrodes on the well floor monitors the activity of overlying cell networks. (C) Sample voltage recording traces from sixteen of the sixty-four electrode sites

Recent advances in human induced pluripotent stem cell (iPSC) technology[9] have pushed MEA-based assays into the mainstream. For example, the FDA's CiPA initiative[10] promotes the use of MEAs to screen pre-clinical drugs for effects on human iPSC derived cardiomyocytes. Similarly, the US Tox21 and European REACH programs have called for increased *in vitro* neural screening[11], an application in which MEA assays are highly sensitive to both neurotoxicity[6,12,13] and proconvulsant effects[14,15]. Moreover, iPSC neurons from diseased patients are now routinely used to create cellular models of neural disorders. The resulting "disease-in-a-dish" models are analyzed with MEAs to provide patient-specific *in vitro* test beds for diseases such as ALS[16], fragile X[17], long QT syndrome[18], and epilepsy[19–21].

Axion's multiwell MEAs enable high throughput and multi-parameter experimentation

In response to the growing applications for functional assessment of excitable cells, Axion Biosystems scaled MEA technology to multiwell plates for high-throughput experiments. The Maestro system provides 768 microelectrodes divided among 12, 48, and 96 wells on a single microplate (Fig. 2). This system allows the user to run parallel experiments to explore multiple variables, such as culture variations (*e.g.* cell density, genetic mutations) or treatment types (*e.g.* candidate drugs, dosages). In contrast, the serial nature of traditional single-well MEA systems makes even basic investigations, at low 'N'-counts, time and cost prohibitive. Axion's SBS-compliant multiwell plates match industry standards, allowing the same cultures to be analyzed with other technologies, including high throughput imaging.
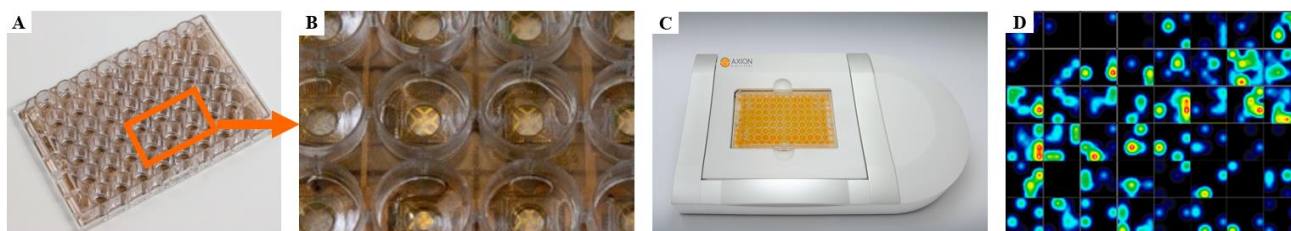
Figure 2: (A, B) Axion's multiwell MEAs dock within (C) the Maestro system. (D) Software display of network activity within each well of a forty-eight well MEA plate

Existing techniques for controlling multiwell MEA cultures are limited

Despite the ability of MEAs to monitor electrical activity, this technology's impact would be greatly enhanced by alternative methods of manipulating cell cultures. Spontaneous network activity is informative, but significant gains in reliability and predictivity may be made through the ability to precisely perturb or probe the network. Towards this end, electrical stimulation is useful, but limited. Current pulses from microelectrodes activate all proximal cell types, and cannot effectively inhibit network components. Furthermore, electrical stimulation can produce artifacts that obscure recordings of critical activity after stimulation.

Optogenetics enables selective control of cell networks

Optogenetics techniques provide the targeted activation and inhibition capability that is critical for exploring complex cell networks[22]. Using standardized techniques and off-the-shelf viral vectors, selected cells can be easily manipulated to express light sensitive membrane proteins (opsins). For example, neurons expressing Channelrhodopsin-2 (ChR2) depolarize and fire action potentials when illuminated[23] with blue light. Other opsins, such as halorhodopsins[24,25] (NpHR) or archaerhodopins[26] (Arch), respond to orange or green light with membrane hyperpolarization, suppressing activity. Recently developed light sensitive G-protein coupled receptors allow precise control over intracellular signaling pathways[27], paving the way towards influence over developing or differentiating cultures through chronic stimulation.

Optogenetic stimulation advances MEA-based models and newly emerging applications

Optogenetic techniques have been critical in characterizing neuronal and cardiac circuits, manipulating developing iPS cells[28] and studying disease[29,22]. From autism[30] and depression[31] to addiction[32], optogenetic-based selective manipulation has enabled the detailed analysis of cellular networks for a wide range of disorders. In recent studies, optogenetic stimulation of MEA cultures demonstrated the power of combining optical control with network-wide electrical monitoring[21,33,34]. For example, pacing electrical activity in cardiomyocyte cultures standardizes activity to reduce assay variability. Targeted activation of specific neuronal cell types provides unique mechanistic information on activity changes. Optical control of MEA cultures also allows exploration of underlying mechanisms of plasticity[21,34] and synchrony[33].

Further, use of optogenetic stimulation is rapidly expanding to new applications, indicating expanded adoption and new market opportunities. For example, optogenetic techniques have been combined with CRISPR for spatiotemporally precise gene modification[35,36], and engineered to control stem cell differentiation[28]. These new optogenetic applications, among others, extend beyond electro-active cells to significantly broaden the impact of *in vitro* optogenetics and motivate high throughput screening.

Integration of optical stimulation capabilities into a multiwell MEA platform

Although optogenetics techniques have produced significant results, to date they have been performed on a single or low-well count basis, using custom, non-scalable, devices for light delivery. Thus, there is a need for a turn-key, multiwell solution. Here, we describe a multiwell optical delivery device, designed in a top-side form factor compatible with simultaneous bottom-side electrical recording or imaging.
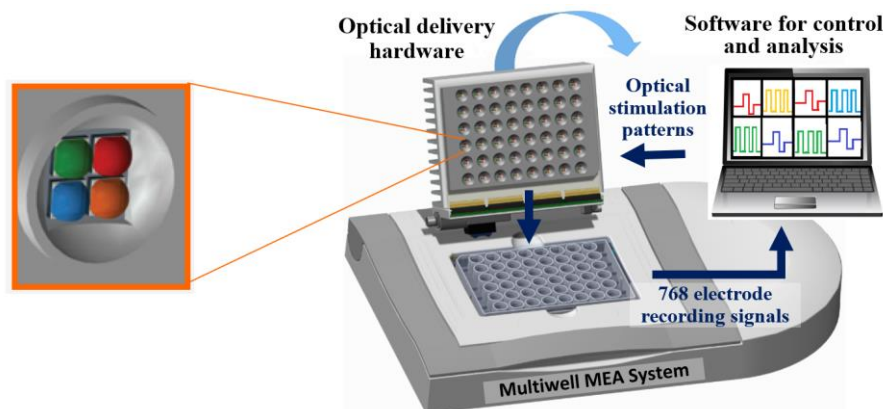
Figure 3. Light delivery is precisely and independently controlled within each well of a multiwell plate in a top-down design compatible with simultaneous MEA recordings or bottom-side imaging

2. METHODS

2.1 Device design

A multiwell optical stimulation device was developed to independently illuminate each well of a standard 48-well microplate. Toward this end, 192 independently addressable LEDs with center wavelengths encompassing the visible spectrum (475nm, 530nm, 612nm, 655nm) were laid out in forty-eight groups of four (Fig. 4A). An array of metallic reflectors was fabricated to concentrate and deliver light from each LED group to the bottom MEA surface of its corresponding well. For precise control over intense light delivery, customized instrumentation was designed around an on board, dual-core CPU with tightly integrated FPGA co-processor. This setup provided independent control of each high intensity LED, at 100μs temporal resolution, with finely graded control over intensity levels for arbitrary irradiation patterns such as intensity ramps. A closed-loop temperature control system was developed around a fan-cooled heatsink (Fig. 4B) to provide cooling and regulation of the microplate lid temperature to 37°C to reduce condensation formation on the microplate lid. The light delivery assembly was designed to fit over a gas delivery base with a ring of outlet ports, providing evenly distributed 5% CO_2 gas to maintain environmental stability during cell culture experiments (Fig. 4C,D).
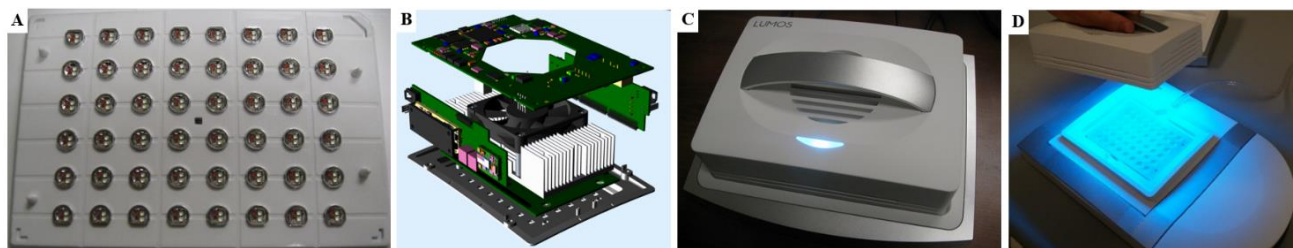
Figure 4. A) Array of 48 LED banks and metallic reflectors. B) Custom control circuitry and active temperature control system. C-D) The light delivery device mates to the lid of a 48-well microplate, forming a seal around a distributed gas delivery system for environmental control.

MEA plates were designed to optimize optical effects. For example, microplate lids contained an embedded array of recessed Fresnel lenses to provide light containment, beam shaping, and mechanical alignment with the LED/reflector array. MEA microplate walls were molded from a custom formulated white, opaque polymer to maximize specular reflection and light delivery, evenly diffuse light within each MEA well, and minimize bleed through of light between adjacent wells. Microplate MEA substrates were comprised of either an opaque FR-4 material or a transparent polymer material. MEA electrodes and traces were gold, and in some cases electropolymerized with Poly(3,4-ethylenedioxythiophene (PEDOT) to reduce electrode impedance.

Light delivery to the MEA surface was quantified using a silicon photodiode (FDS1010, ThorLabs) biased at 5V, during 1ms, 1Hz test pulses at controlled currents. EMI noise and optoelectric artifact were investigated during simultaneous voltage recordings using Axion's AxIS software analysis system.
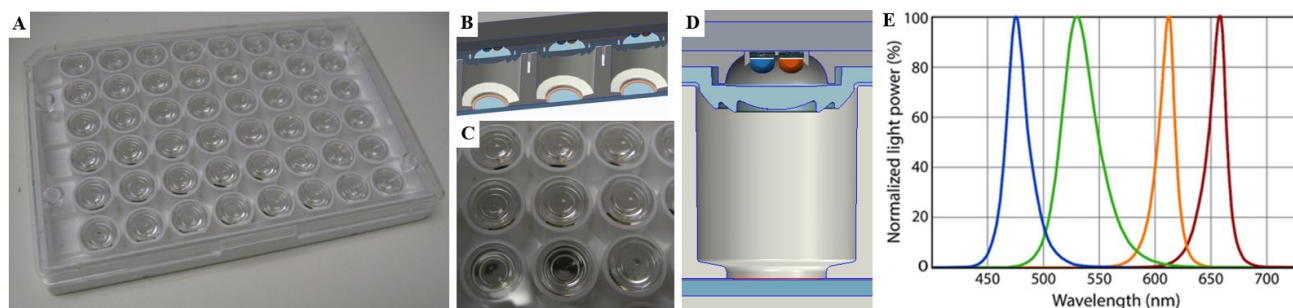
Figure 5. A-D) Optically specialized microplate with high-reflectance polymer wells and a lid containing an array of recessed lenses. E) Four LEDs in each well cover the visible spectrum for targeting of multiple opsins.

2.2 Software for light generation, visualization, and analysis

Axion's AxIS software suite was modified to enable graphical-based generation of light patterns and targeting of desired wells (Fig. 6A). Visualization panels were supplemented to display markers of delivered light pulses overlaid on running plots of recorded electrical cell activity (Fig. 6B). Synchronization pulses enabled precise alignment of light delivery with recordings of electrophysiological activity. For advanced analysis of evoked activity at the multiwell level, a custom MATLAB-based software tool was developed (Neural Metric Tool, Axion Biosystems, Inc.). This tool computed the magnitude, probability, latency, and precision of the neural response across repeated presentations of the stimulus.
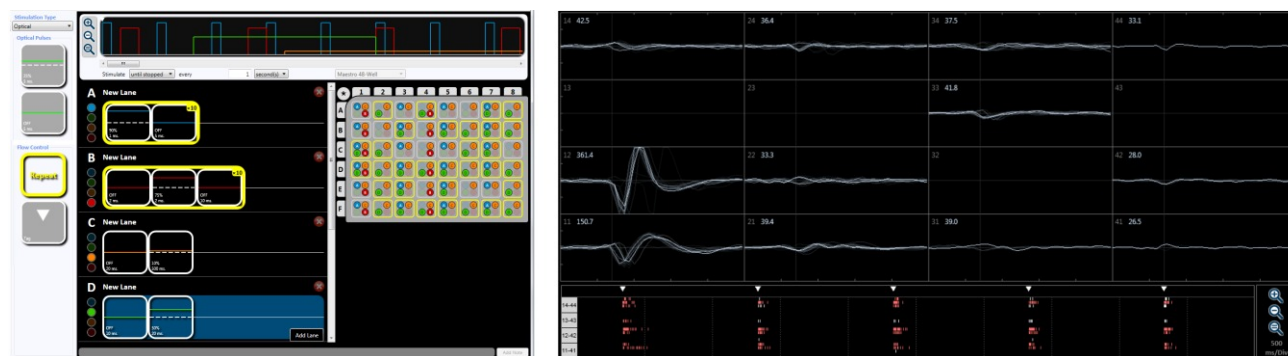
Figure 6. A) Screenshot of optical generation tools. Multiple light patterns can be graphically designed and targeted to specific MEA wells. B) Screenshot of visualization of optical delivery overlaid onto electrical recordings. White triangular markers denote the timing of light delivery pulses within a real-time raster plot of detected spikes on each electrode (bottom).

2.3 Cell culture and viral transduction

MEA Preparation:

MEA plates were prepped for cell culture by first spotting surface coatings onto the MEA surfaces. Polyethylenimine (PEI) at 0.1% was used to coat each MEA (5µL drop size) before incubating the plate for 1 hour at 37°C. After incubation, each well was rinsed four times with 200µL of deionized water and allowed to dry overnight in a biosafety cabinet. Laminin (10µg/mL) was then spotted into each well (5µL drop size) and incubated for 1 hour at 37°C.

Cell culture protocols:

Rat cortical neurons (QBM Cell Science, cat. no. R-CX-500) were plated at 160,000 cells per well (5μL drop size) into the 48-well MEA plates. Neurons were cultured in Neurobasal media (Thermofisher, #21103-049) supplemented with B-27 (Thermofisher, #A1895601) for 30 days, with 50% media changes performed every 3 days. Initial recordings were conducted after 14 days *in vitro (DIV14)* to allow networks to develop and spontaneous synchronized bursting events to emerge. Subsequent baseline recordings were taken weekly, at least 24 hours after a media change.

Human iPSC-derived cardiomyocytes (Cellular Dynamics International, iCell CM^2) were plated at 50,000 cells per well (5μL drop size). Full media changes were performed every 2 days. Recordings were taken at least 4 hours following a media change, evaluating electrode coverage, sodium spike amplitude, and t-wave coverage and shape.

Experiments at Columbia University were performed with using primary mouse cortical neurons. Whole neocortex was dissected from C57Bl6/J post-natal day 0 (P0) mice and digested in 0.25% trypsin (LifeTechnologies, #25200). After enzymatic digestion, cells were mechanically dissociate by aspirating through a conical pipette tip and diluted to 6000 cells per microliter. Cells were plated at a density of 150,000 cells per 25 μl drop into the 48-well MEA plates. Neurons were cultured in Neurobasal-A media (Gibco, 10888) supplemented with B-27 (Gibco, 17504), HEPES, and Penicillin-Streptomycin for 24 days with media changes performed every other day starting on day 12.

Viral transduction:

Neurons and cardiomyocytes were transduced to induce expression of Channelrhodopsin-2 (ChR2) or Archaerhodopsin T (ArchT) along with a green fluorescent protein (GFP) (UNC Vector Core) via an AAV-9 viral vector and CAG promoter.

ChR2 = rAAV9/CAG-ChR2-GFP viral vector (3.9x10^{12} viral molecules/mL)
ArchT = rAAV9/CAG-ArchT-GFP viral vector (3x10^{12} viral molecules/mL)

The viral vector was added either to the cell suspension during plating, or to individual wells 2-5 days after the cultured networks were established. Transduction in the cell suspension during plating was achieved by adding 400nL/well, whereas 3μL/well was required for transduction in individual wells at 2-5 days *in vitro*. Optogenetic experiments were performed at least 7 days after transduction to allow for sufficient expression of the opsins.

2.4 MEA experiments

Optogenetic MEA experiments were performed using the Maestro multiwell MEA platform (Axion Biosystems, Inc.) and the Lumos light delivery system (Axion Biosystems, Inc). Media was exchanged at least 4 hours in advance of electrophysiological experiments to minimize mechanical and chemical perturbations to the cells. For dosing experiments, each well received a single concentration of a test compound or control. Compounds were prepared at 10x the intended concentration and added to the well in a 1:10 dilution. Recordings were acquired and analyzed using the AxIS software suite (Axion Biosystems, Inc).

3. RESULTS AND DISCUSSION

3.1 Device characterization

Each of the 192 LEDs could be modulated independently with sub-microsecond rise times and 100μs update rates (Fig. 7C,D) with a linear relationship between control current and measured light outputs (Fig. 7B). Irradiance across the MEA culture sites was quantified with a calibrated photometer (Fig. 7A) and was also found empirically to exceed threshold values necessary for robust optogenetic response (Fig. 9B). Standard culture media containing phenol red dye found in culture media was found to attenuate light delivery, particularly for the blue and green wavelengths. Commercially available culture media without Phenol red dye can be used during optical stimulation protocols, but this was not necessary due to the available light delivery intensity.

The temperature control system was able to maintain LED device temperatures to a set target with better than 1°C accuracy. A target temperature of 37° C at the LED reflector was chosen to match the temperature of the underlying microplate heater. Regulating the temperature above and below the MEA eliminated undesired temperature gradients across the MEA. Eliminating the temperature differential prevented liquid condensation on the microplate lid, which was observed to otherwise build up over time.
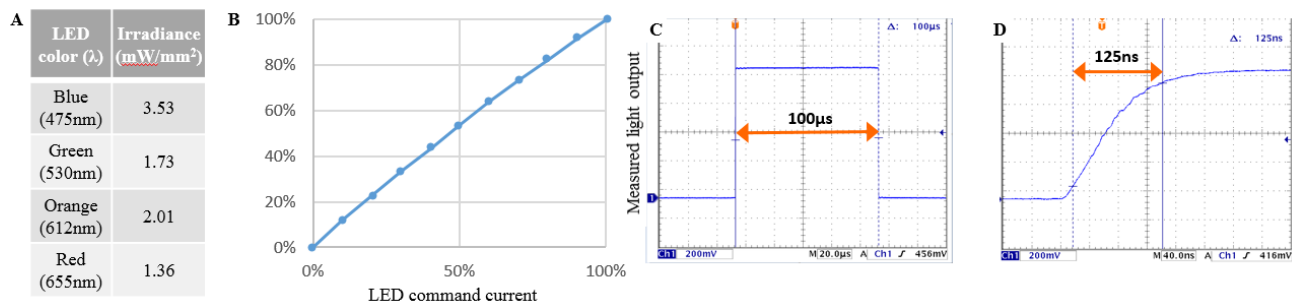
Figure 7. Optical delivery hardware characterization. A) Measured light delivery to MEA surface B) LED control signal vs. measured output for a representative blue LED C) 100µs pulse measured from a representative blue LED D) 10-90% rise time for the leading pulse edge was measured at125ns

The gas delivery system was tested over time by observation of 1) pH change (measured by media color change over time) and 2) beat rate of cardiac cell cultures over time. Both metrics confirmed a stable environment for the cell cultures with the control systems in place during extended experiments.

PEDOT coatings effectively reduced gold electrode impedances, lowering from an average of 1.04 MΩ at 1 kHz to 25.9 kΩ. Transparent-bottomed MEA plates could be clearly imaged with an inverted microscope, allowing assessment of culture viability, distribution, and GFP expression.

3.2 Validation of multiwell optogenetics for activation and suppression of neural activity

The system was validated through optogenetic experiments with rodent cortical cultures. Fluorescent imaging of cultures on transparent-bottomed microplates confirmed robust opsin expression through co-localized GFP tags (Fig. 8A). Cultures were viable and distributed in close proximity to MEA recording electrodes. Functional expression was tested by assessing extracellular action potential firing in response to blue light pulses for ChR2-expressing wells and extended pulses of green light for ArchT-expressing wells. Figure 8B illustrates a typical response to blue light for a ChR2-expressing cell, with a single action potential elicited by each pulse of light (5ms pulse duration). By contrast, ArchT, a light-activated proton pump, suppressed action potential firing during green light delivery (Fig. 8C). Neural activity was quantified before, during, and after optogenetic stimulation for ChR2-expressing wells to verify that the light stimulus did not affect the spontaneous activity of the network (Fig. 8D).

As a final control and validation of multiwell light delivery, neural cultures were plated in all wells of a 48-well MEA plate. Twenty-four of the wells were transduced with ChR2, while the remaining twenty four wells were left as untreated controls. Optically-evoked activity was quantified across the plate. In Fig. 8E, the shading of each well in the plate map provides a quantitative measure of the evoked activity, averaged across 50 repeats of a blue light pulse (5ms duration, 50% light intensity). As expected, the 24 ChR2+ wells in the top half of the plate exhibited a response that was robust and consistent across wells and tightly correlated with delivered light pulses. Control wells exhibited insignificant evoked activity. The example raster plots (Fig. 8E, middle) for a ChR2+ well (top) and a control well (bottom) illustrate typical network responses. For the ChR2+ well, each pulse of blue light initiated a burst of network activity that was consistent across repetitions.

A peri-stimulus time histogram (PSTH) and peri-event raster were produced by averaging the network response of the culture across repetitions of the light stimulus (Fig. 8E, right). The peri-event raster (bottom) illustrates that the majority of the electrodes in the well detect neural activity at a short latency after the stimulus, with minimal jitter across trials. The PSTH (top), which sums activity across electrodes in the peri-event raster, serves as the basis for computation of evoked activity metrics, such as the magnitude, latency, and precision of the neural response. Evoked activity metrics add a new dimension to phenotypic investigation of neural cultures, which may improve sensitivity of toxicological assays or aid functional characterization of genetic mutations in models of neural disease, such as epilepsy.
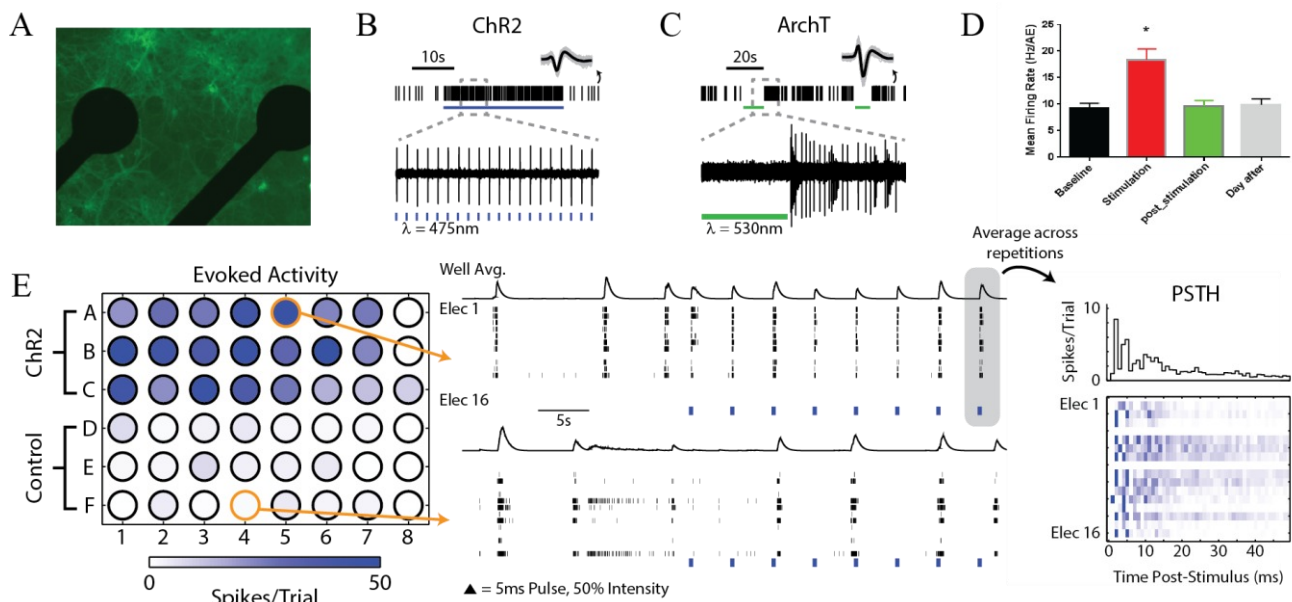
Figure 8. Validation of multiwell optogenetics for activation and suppression of neural activity. A) Fluorescent micrograph of mouse cortical neuron cultures (20X). Response of individual neurons to pulses of B) blue light (475nm) for ChR2^{+} and C) green light (530nm) ArchT^{+} cells. D) Network activity was not affected long-term by the stimulation of ChR2. E) Exemplary neural response data from a plate, demonstrating simultaneous multiwell stimulation. Left: Plate map showing levels of evoked activity. Middle: Raster plots from representative wells. Right: Peri-stimulus time histograms, averaged across stimulus repeats from a sample well.

3.3 Optogenetic control of neural network activity for enhanced neurotoxicity screening

Evoked metrics may lead to improved sensitivity and reliability of existing *in vitro* neural assays, such as proconvulsant risk assessment. As a simple proof of concept, we characterized evoked response metrics (Fig. 9A) as a function of light intensity before and after dosing. In baseline, the response magnitude (Fig. 9B) increased with light intensity before reaching saturation at 10% light intensity from the device, supporting that the light output of the Lumos is sufficient for neural optogenetic experiments. The response probability (Fig. 9C) also saturated at 10% light intensity, while the jitter (Fig. 9D) in the evoked neural response decreased until saturating at 30% light intensity.
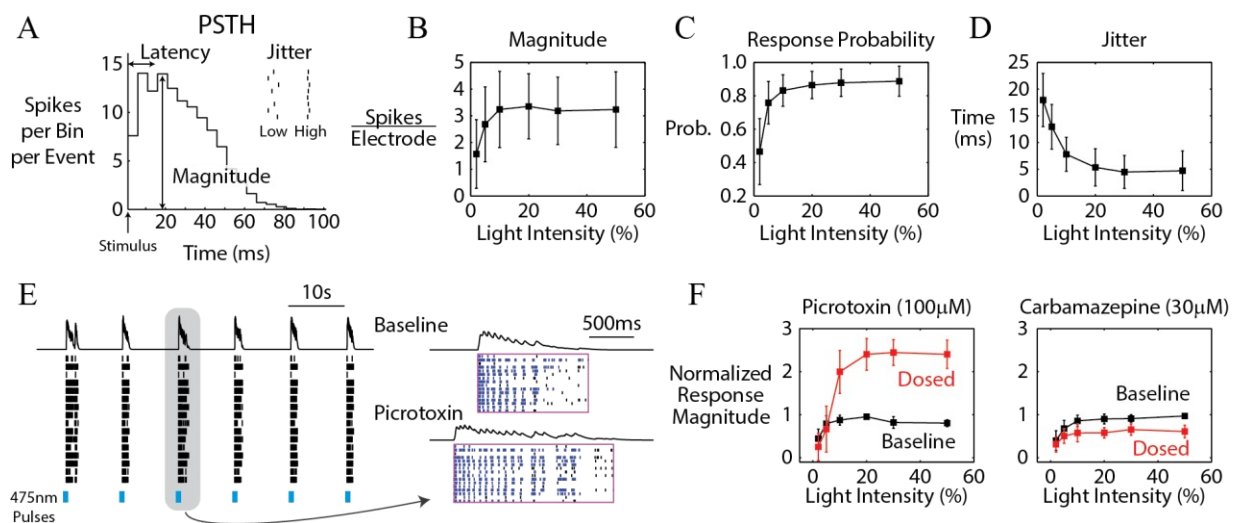
Figure 9. Quantification of optically-evoked neural activity for screening applications. A) Metrics of optically-evoked neural activity are extracted from the peri-stimulus time histogram (PSTH) and peri-event raster plot. The B) magnitude, C) probability, and D) jitter of the neural response are directly modulated by the strength of the light stimulus. E) ChR2-expressing neural cultures dosed with picrotoxin exhibited prolonged network bursts following stimulation with blue light. F) Picrotoxin significantly increased the magnitude of optically-evoked neural activity, while carbamazepine suppressed evoked activity.

Evoked metrics were sensitive to the addition of neuro-active compounds, such as picrotoxin and carbamazepine. Each pulse of blue light elicited a burst of activity, which increased in magnitude and duration in response to picrotoxin addition (Fig. 9E). For each well, the magnitude of the evoked response was normalized to the response at the highest light intensity, and compared for baseline and dosed conditions (Fig. 9F). Picrotoxin, a known proconvulsant, elicited an increase magnitude in the evoked response, while carbamazepine, a common anti-epileptic drug, significantly reduced the magnitude in the evoked response. By reducing variability across wells, and enabling new phenotypic measures of neural activity, evoked activity may improve the sensitivity of neurotoxicity and drug safety assays.

3.4 Optogenetic pacing of cardiac beat rate for enhanced drug screening with human-derived iPSC cardiomyocytes

The multiwell light delivery system was also validated using human iPSC-derived cardiomyocytes expressing ChR2 (Fig. 10A). Regularly timed pulses of blue light were sufficient to optically pace cardiac cultures faster than the spontaneous beat rate. An example of the onset of pacing is shown in Fig. 10B, illustrating the instantaneous change in beat period as the light pulses entrain the cardiac beating frequency. ChR2 expression increased over time *in vitro*, such that all wells could be paced with 5ms pulses at 20% light intensity on DIV7 and 8% light intensity on DIV12.

At DIV12, the pacing rate was varied systematically to evaluate the relationship between beat rate and repolarization in human iPSC-derived cardiomyocytes. Example paced field potential traces are shown in Fig. 10D for a range of paced beat periods in a single well. As expected, the field potential duration shortened with increasing pacing rate. The relationship between beat period and field potential duration, as shown in Fig. 10E, was highly consistent across wells in the plate (N=24; gray, individual wells; black, Bazett formula). Evaluation of the relationship between beat period and field potential duration allows the estimation of a custom rate-correction function for each plate, or for the investigation of rate-dependent electrophysiological phenomena.

In addition to the field potential duration, the presence of early after-depolarizations (EADs) was sensitive to the beating frequency of the cell network (Fig. 10F). Addition of sotalol (10μM) produced EADs on every beat at the spontaneous beat period (1560ms, top). The EADs progressively disappeared as the pacing rate was increased (middle), with no EADs present at a paced beat period of one second. Thus, optogenetic stimulation can be used to control for emergent arrhythmic events, or more precisely quantify cardiac arrhythmias.
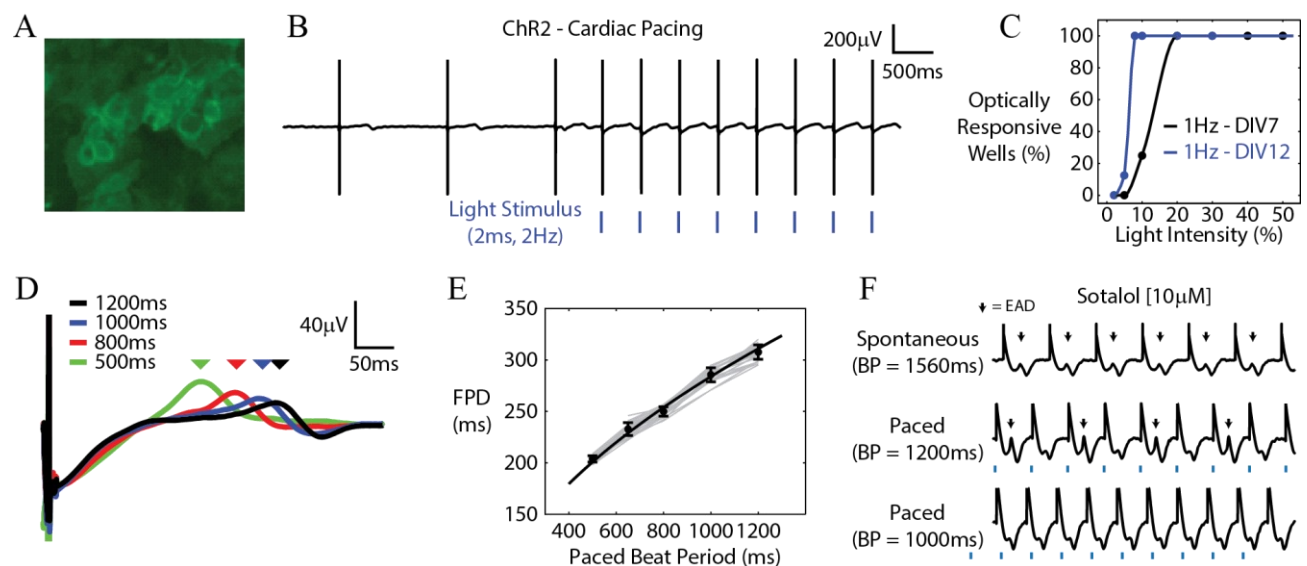
Figure 10. Optogenetic techniques for multiwell pacing of stem cell derived cardiomyocytes. A) Fluorescence microscopy verified expression of ChR2 through co-located GFP labeling. B) Example cardiac field potential in response to optical pacing of the culture beat rate. C) Percent of optically-paced wells, as a function of light intensity, on days 7 (black) and 12 (blue) after transduction. D) The field potential duration (triangles) decreased for increasing pacing rates. E) The relationship between field potential duration and beat period was highly repeatable across cardiomyocyte cultures in a plate (individual wells, gray lines; mean, black dots; errors bars indicate standard deviation across wells). F) Arrhythmic events, like EADs (arrows), were also systematically modulated by pacing rate in the presence of sotalol (10μM).

4. CONCLUSION

These experiments validate the function of a multiwell optical delivery device and demonstrate its potential to enhance multiwell MEA-based assays. The device was shown to independently deliver precisely controlled levels of robust optical stimulation at selectable wavelengths to 48 MEA wells. Sample neural- and cardiac-based applications were validated in proof-of-concept demonstrations.

Future device work will expand to higher well counts (*e.g.* 96 wells) and development of enhanced control and analysis software for application specific functionality. Future experimentation will explore advanced applications, such as cell-type specific modulation in heterogeneous disease-in-a-dish models, closed-loop paradigms for tuning of network activity states, and chronic light delivery for influence over cell culture development or differentiation.

REFERENCES

[1]   Thomas, C. A., Springer, P. A., Loeb, G. E., Berwald-Netter, Y. & Okun, L. M. "A miniature microelectrode array to monitor the bioelectric activity of cultured cells," *Exp. Cell Res.* **74,** 61–6 (1972).

[2]   Stett, A. *et al.* "Biological application of microelectrode arrays in drug discovery and basic research," *Anal. Bioanal. Chem.* **377,** 486–95 (2003).

[3]   Dunlop, J., Bowlby, M., Peri, R., Vasilyev, D. & Arias, R. "High-throughput electrophysiology: an emerging paradigm for ion-channel screening and physiology," *Nat. Rev. Drug Discov.* **7,** 358–68 (2008).

[4]   Chiappalone, M. *et al.* "Networks of neurons coupled to microelectrode arrays: a neuronal sensory system for pharmacological applications," *Biosens. Bioelectron.* **18,** 627–34 (2003).

[5]   Easter, A. *et al."* Approaches to seizure risk assessment in preclinical drug discovery," *Drug Discov. Today* **14,** 876–84 (2009).

[6]   Johnstone, A. F. M. *et al.* "Microelectrode arrays: a physiologically based neurotoxicity testing platform for the 21st century," *Neurotoxicology* **31,** 331–50 (2010).

[7]   Meyer, T., Boven, K.-H., Günther, E. & Fejtl, M. "Micro-electrode arrays in cardiac safety pharmacology: a novel tool to study QT interval prolongation," *Drug Saf.* **27,** 763–72 (2004).

[8]   Wagenaar, D. A., Pine, J. & Potter, S. M. "An extremely rich repertoire of bursting patterns during the development of cortical cultures," *BMC Neurosci.* **7,** 11 (2006).

[9]   Takahashi, K. *et al.* "Induction of pluripotent stem cells from adult human fibroblasts by defined factors," *Cell* **131,** 861–72 (2007).

[10]   Sager, P. T., Gintant, G., Turner, J. R., Pettit, S. & Stockbridge, N. "Rechanneling the cardiac proarrhythmia safety paradigm: A meeting report from the Cardiac Safety Research Consortium," *Am. Heart J.* **167,** 292–300 (2014).

[11]   Marchan, R., van Thriel, C. & Bolt, H. M. "Recent developments in in vitro toxicology: perspectives of European research and Tox21," *Arch. Toxicol.* **87,** 2043–6 (2013).

[12]   Defranchi, E. *et al.* "Feasibility Assessment of Micro-Electrode Chip Assay as a Method of Detecting Neurotoxicity in vitro," *Front. Neuroeng.* **4,** 6 (2011).

[13]   Mack, C. M. *et al.* "Burst and principal components analyses of MEA data for 16 chemicals describe at least three effects classes," *Neurotoxicology* **40C,** 75–85 (2013).

[14]   Colombi, I., Mahajani, S., Frega, M., Gasparini, L. & Chiappalone, M. "Effects of antiepileptic drugs on hippocampal neurons coupled to micro-electrode arrays," *Front. Neuroeng.* **6,** 10 (2013).

[15]   Vedunova, M. *et al.* "Seizure-like activity in hyaluronidase-treated dissociated hippocampal cultures," *Front. Cell. Neurosci.* **7,** 149 (2013).

[16]   Dimos, J. T. *et al.* "Induced pluripotent stem cells generated from patients with ALS can be differentiated into motor neurons," *Science* **321,** 1218–21 (2008).

[17]   Liu, J. *et al.* "Signaling defects in iPSC-derived fragile X premutation neurons," *Hum. Mol. Genet.* **21,** 3795–805 (2012).

[18]   Itzhaki, I. *et al.* "Modelling the long QT syndrome with induced pluripotent stem cells," *Nature* **471,** 225–9 (2011).

[19]   Zhu, X., Need, A. C., Petrovski, S. & Goldstein, D. B. "One gene, many neuropsychiatric disorders: lessons from Mendelian diseases," *Nat. Neurosci.* **17,** 773–81 (2014).

[20]   Dhindsa, R. S. & Goldstein, D. B."Genetic Discoveries Drive Molecular Analyses and Targeted Therapeutic

Options in the Epilepsies," *Curr. Neurol. Neurosci. Rep.* **15,** 70 (2015).

[21] Lignani, G. *et al."* Long-term optical stimulation of channelrhodopsin-expressing neurons to study network plasticity," *Front. Mol. Neurosci.* **6,** 22 (2013).

[22] Tye, K. M. & Deisseroth, K. "Optogenetic investigation of neural circuits underlying brain disease in animal models," *Nat. Rev. Neurosci.* **13,** 251–66 (2012).

[23] Boyden, E. S., Zhang, F., Bamberg, E., Nagel, G. & Deisseroth, K. "Millisecond-timescale, genetically targeted optical control of neural activity," *Nat. Neurosci.* **8,** 1263–8 (2005).

[24] Gradinaru, V., Thompson, K. R. & Deisseroth, K. "eNpHR: a Natronomonas halorhodopsin enhanced for optogenetic applications," *Brain Cell Biol.* **36,** 129–39 (2008).

[25] Gradinaru, V. *et al.* "Molecular and cellular approaches for diversifying and extending optogenetics," *Cell* **141,** 154–65 (2010).

[26] Chow, B. Y. *et al.* "High-performance genetically targetable optical neural silencing by light-driven proton pumps," *Nature* **463,** 98–102 (2010).

[27] Airan, R. D., Thompson, K. R., Fenno, L. E., Bernstein, H. & Deisseroth, K. "Temporally precise in vivo control of intracellular signalling," *Nature* **458,** 1025–1029 (2009).

[28] Sokolik, C. *et al.* "Stem Cells to Distinguish Authentic Signals from Transcription Factor Competition Allows Embryonic Stem Cells to Distinguish Authentic Signals from Noise," *Cell Syst.* **1,** 117–129 (2015).

[29] Tønnesen, J. "Optogenetic cell control in experimental models of neurological disorders," *Behav. Brain Res.* **255,** 35–43 (2013).

[30] Yizhar, O. "Optogenetic insights into social behavior function," *Biol. Psychiatry* **71,** 1075–80 (2012).

[31] Covington, H. E. *et al.* "Antidepressant effect of optogenetic stimulation of the medial prefrontal cortex," *J. Neurosci.* **30,** 16082–90 (2010).

[32] Stamatakis, A. M. & Stuber, G. D. "Optogenetic strategies to dissect the neural circuits that underlie reward and addiction," *Cold Spring Harb. Perspect. Med.* **2,** (2012).

[33] El Hady, A. *et al.* "Optogenetic stimulation effectively enhances intrinsically generated network synchrony," *Front. Neural Circuits* **7,** 167 (2013).

[34] Tchumatchenko, T., Newman, J. P., Fong, M. & Potter, S. M. "Delivery of continuously-varying stimuli using channelrhodopsin-2," *Front. Neural Circuits* **7,** 184 (2013).

[35] Polstein, L. R. & Gersbach, C. A. "A light-inducible CRISPR-Cas9 system for control of endogenous gene activation," *Nature Chem. Bio.* **11** 198-200 (2015).

[36] Nihongaki, Y., Kawano, F., Nakajima, T. & Sato, M. "Photoactivatable CRISPR-Cas9 for optogenetic genome editing Photoactivatable CRISPR-Cas9 for optogenetic genome editing," *Nature Biotech.* **33**, 755-760 (2015).